

Facile Visible-Light-Assisted Synthesis, Optical, and Electrochemical Properties of Pd Nanoparticles with Single-crystalline and Multiple-twinned Structures

Tan Dexin¹, Wang Yanli², Gan Ying¹

¹Anhui University of Science and Technology, Huainan 232001, China; ² Post-doctoral Research Station, Anhui University of Science and Technology, Huainan 232001, China

Abstract: A facile visible-light-assisted method has been demonstrated to synthesize palladium (Pd) nanoparticles (NPs) with single-crystalline multiple-twinned structures by reduction of PdCl₂. The structures and electrochemical properties of Pd NPs were investigated by high resolution transmission electron microscopy (HRTEM), UV-visible spectroscopy, and cyclic voltammetry (CV). The results show that the formation of different nanostructures depends on the control of reduction rate. Unlike multiple-twinned Pd NPs, single-crystalline Pd NPs exhibit surface plasmon resonance (SPR) peaks in the visible region. By comparison of the electrochemical parameters in the oxidation process of Pd NPs with single-crystalline and multiple-twinned structures, multiple-twinned Pd NPs exhibit the better electrocatalytic activity and anti-poisoning capability for ethanol oxidation.

Key words: nanoparticles; optical properties; electrochemical property; energy-saving lamp

As a noble metal, Pd serves as the primary catalyst for alkene hydrogenation^[1], alcohol oxidation^[2], Suzuki-Miyaura^[3], and Heck reactions^[4]. Moreover, surface plasmon resonance (SPR), as another unusual feature of Pd, could lead to applications in colorimetric sensing, plasmonic waveguiding, and optical sensing of hydrogen^[5]. The properties of metal nanostructures are decided not only by the portion of surface atoms but also by surface structures. The former is directly related to the metal size and the latter depends on the metal shape. It is well known that the catalytic reactions preferentially take place on surfaces of nanoparticles (NPs), and the catalytic activity of metal NPs is highly associated with the structure of facets enclosing the NPs^[6]. Thus, shape-controlled synthesis of metal nanomaterials becomes a promising direction for precisely tailoring their chemical activity, selectivity, and stability. To date, Pd NPs of various morphologies^[7-9] have been successfully prepared. However, a great challenge still remains to find a facile method to fabricate specific Pd

nanostructures.

Recently, photochemical and irradiation synthesis has been proven to be a promising route for the synthesis of various NPs^[10]. Current photochemical methods focus mainly on the use of high-energy radiation, such as UV light or γ -irradiation^[11, 12]. Therefore, it is extremely important to design a safer, cheaper, and more facile light-assisted method for nanomaterials. Retna Raj^[13] has presented a facile photochemical route for the synthesis of triangular Ag nanoplates using sunlamp, and the result demonstrated that light can induce shape transformation of Ag nanoplates.

Based on the fact that Ag nanoplates could be obtained using the sunlamp, we have presented a novel visible-light-assisted method to synthesize Pd NPs. In the present paper, we demonstrate, for the first time, that using palladium chloride (PdCl₂) as the Pd precursor, ethanol as reducing agent and poly(vinyl pyrrolidone) (PVP) as a stabilizer and a guiding agent, Pd NPs with single-crystalline

Received date: August 13, 2016

Foundation item: National Nature Science Foundation of China (51303005); the Educational Commission of Anhui Province of China (KJ2013A087, KJ2013A095)
Corresponding author: Wang Yanli, Ph. D., Professor, School of Materials Science and Engineering, Anhui University of Science and Technology, Huainan 232001, P. R. China, Tel: 0086-554-6668649, E-mail: ylwang1998@163.com

Copyright © 2017, Northwest Institute for Nonferrous Metal Research. Published by Elsevier BV. All rights reserved.

and multiple-twinned structures were selectively synthesized using a facile visible-light-assisted method with a commercial energy-saving lamp as light source. These single-crystalline Pd NPs exhibits unusual optical properties and their SPR peak is located at 520 nm. Moreover, multiple-twinned Pd NPs exhibit remarkable electrocatalytic behavior for ethanol oxidation in 1 mol/L KOH and appear as a promising candidate for use in direct ethanol fuel cells.

1 Materials and Methods

1.1 Materials

PdCl₂ and ethanol were obtained from Nanjing Chemical Reagent No. 1 Factory. PVP was purchased from Sinopharm Chemical Reagent Co. Ltd. All other chemicals were of analytical grade and used as received. All the aqueous solutions were prepared with twice-distilled water.

1.2 Synthesis of single-crystalline Pd NPs

A solution of 1.69×10^{-5} mol PdCl₂ and 1.69×10^{-6} mol PVP were mixed with 4.0×10^{-3} L of ethanol and 2.0×10^{-2} L of deionized water in a 1×10^{-1} L glass vessel. The mixture was dispersed to form a homogeneous solution by constant strong stirring for 2 h. Then, the mixture was irradiated for 6 h with visible light from the 85-Watt energy-saving lamp at a distance of 5 cm. The brown suspension was precipitated by acetone and washed with ethanol three times to remove excess PdCl₂ and PVP. The final brown product could be easily redispersed in ethanol to yield a clear homogeneous solution.

1.3 Synthesis of multiple-twinned Pd NPs

The experimental setup and the procedure were similar to what were used for the single-crystalline Pd nanomaterials, except that the mixture was irradiated for 70h with visible light from the 9-Watt energy-saving lamp at a distance of 5 cm.

1.4 Characterization

The high resolution transmission electron microscopy (HRTEM) observation and the fast Fourier transformation (FFT) were performed with a Tecnai G2 F20 instrument. The powder X-ray diffraction (PXRD) pattern was recorded on a XRD-6000 diffractometer employing Cu K α radiation. The UV-visible spectroscopy of the samples was obtained by an UV-visible spectrophotometer (UV-2600) from Shimadzu. The intensity of the light was detected by a FZ400 visible light power meter.

1.5 Electrochemistry tests

Electrochemical measurements were performed with a CHI 660E electrochemical workstation (CH Instruments, Chenhua Co., Shanghai, China), and conducted on a conventional three-electrode cell, which includes a platinum wire as counter electrode, a saturated calomel electrode (SCE) as reference electrode and the Pd-modified glassy carbon electrode (GCE, 3mm in diameter) as working electrode. For the preparation of the Pd nanomaterials modified

electrode, 5 μ L suspension containing Pd nanomaterials was dropped on the clean electrode surface and dried in air. Next, the Nafion film was prepared by dropping 3 μ L Nafion solution (0.1 wt%) onto the electrode and allowed the solvent to evaporate at room temperature. CVs of the Pd nanomaterials modified electrode were recorded in 1 mol/L KOH solution containing 1 mol/L ethanol. The solutions were deaerated thoroughly for at least 30 min with pure nitrogen gas and kept under a positive pressure of this gas during the experiments.

2 Results and Discussion

In this work, the experimental setup is shown in Fig.1. The suspension changed its color from yellow to brown after it had been irradiated for 6 h with visible light from the 85-Watt energy-saving lamp at a distance of 5 cm (6.63 mW cm⁻² put on the reacting mixture).

Fig.2a shows the TEM images of a typical product which contains hexagonal and triangular single-crystalline Pd NPs of (19 \pm 1) nm in size along with few quasi-spherical NPs (~4 nm). The edge length of hexagonal nanoparticle is not identical and it varies between 10 and 12 nm (Fig.2b). The FFT (inset of Fig.2b) at higher magnification reveal two main diffraction rings, $d_1=0.225$ nm and $d_2=0.198$ nm corresponding to the (111) and (200) plane lattices of cubic Pd, respectively. A typical triangular Pd nanoparticle has an edge length of 23 nm (Fig.2c). The FFT (inset of Fig.2c) also reveals two diffraction rings, the (111) and (200) plane lattices of cubic Pd.

Fig.3 shows the typical PXRD pattern of as-prepared Pd NPs. All the peaks can be assigned to the characteristic peaks of fcc Pd (JCPDS card, 05-0681). It is notable that the ratio between the intensities of (111) and (200) peaks is higher than the index value (3.07 versus 2.38), indicating that the top and bottom faces of each nanoparticle are bounded by {111} planes. As discussed by Xiong^[14], these single-crystalline Pd NPs have a stronger (111) diffraction peak than conventional samples because they should be more or less oriented parallel to the supporting substrate.



Fig.1 Experimental setup of the visible-light-assisted method

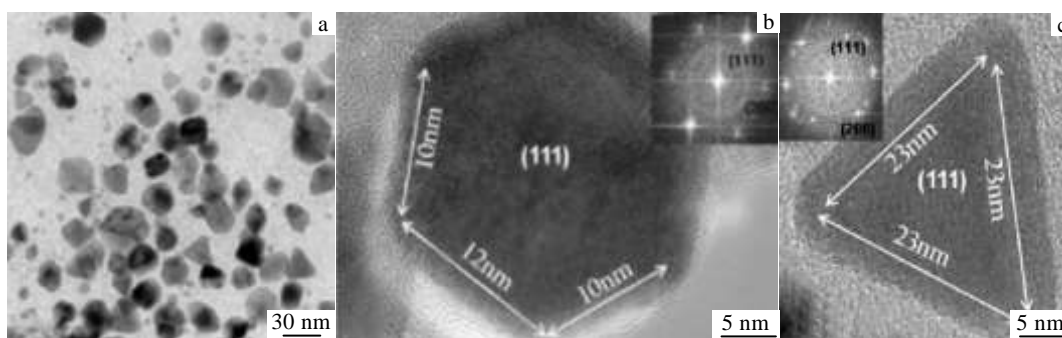


Fig. 2 TEM image of single-crystalline Pd NPs (a); HRTEM image of a typical hexagonal Pd and its corresponding FFT (b); HRTEM image of a typical triangular Pd and its corresponding FFT (c)

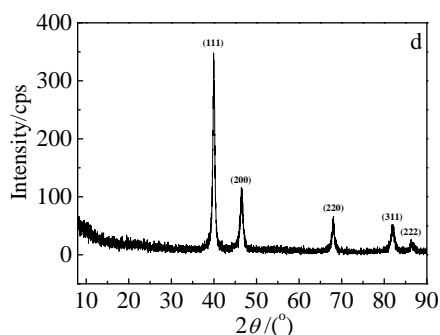


Fig. 3 PXRD pattern of as-prepared sample

On the basis of the fact that formation of highly anisotropic nanostructures only becomes favorable in a slow reduction process, the reduction kinetics should be carefully controlled in order to obtain different Pd nanostructures^[14]. When the reaction mixture was irradiated with a 9-Watt energy-saving lamp after 70 h of slow irradiation (0.37 mW cm^{-2} put on the reacting mixture), fewer single-crystalline Pd NPs were observed and more multiple-twinned Pd NPs were seen (see Fig. 4a). So the critical role of reduction rate in controlling nanostructures was confirmed. These multiple-twinned NPs were reported for Ag to exhibit generally five-fold symmetry^[15]. In this study, a relatively high proportion of multiple-twinned Pd NPs formed with six subunits, which has a mean dimension of $(20 \pm 1) \text{ nm}$, was observed (Fig. 4b). The FFT (inset of Fig. 4b) reveals two main diffraction rings. The reciprocal distances find $d_1 = 0.225 \text{ nm}$ and $d_2 = 0.199 \text{ nm}$ corresponding to the (111) and (200) plane lattices of cubic Pd, respectively. Although the detailed formation mechanism of the multiple-twinned structures is currently unknown, Xie^[16] suspect that both the stacking fault and intrinsic equilibrium structures of lower energy could lead to those multiple-twinned nanostructures.

Since the SPR peaks of Pd NPs (typically $<10 \text{ nm}$ in size) are located in the UV region, the SPR properties of Pd NPs

remain largely unexplored^[14,17]. Fig. 5 shows UV-vis spectroscopy taken from suspensions of the Pd NPs. Different from the multiple-twinned Pd NPs (Fig. 5b), single-crystalline Pd nanomaterials exhibit SPR peaks in the visible region. Their SPR peaks are located at 520 nm and become very broad (Fig. 5a). The exceptional wide range of wavelength across which single-crystalline Pd NPs strongly absorb light should make them potentially useful as nanoscale photothermal heating elements^[18].

It is well known that Pd has been demonstrated to be very active and even more efficient than Pt for ethanol oxidation in alkaline medium rather than acidic media. As a matter of fact, several advantages are attached to ethanol oxidation on Pd: firstly, ethanol is non-toxic and can be synthesized in

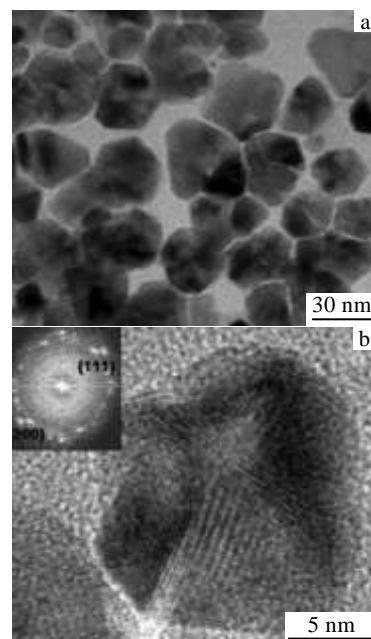


Fig. 4 TEM image of multiple-twinned Pd NPs (a); HRTEM image of a polyhedral particle formed with six tetrahedral subunits and its corresponding FFT (b)

large quantities from glucose-containing biomass, and secondly, Pd is much cheaper and is 50 times more abundant than Pt in ores^[19].

Fig. 6 shows the voltammogram run of the Pd nanomaterials modified GCE and bare GCE in the oxidation of ethanol in alkaline medium. Except for bare GCE, the single-crystalline and multiple-twinned Pd nanomaterials modified GCE exhibit electrocatalytic activity for ethanol oxidation in alkaline medium. The main characteristics which can be measured from such voltammograms include: E_{onset} is the faradaic current onset potential; E_f is the forward peak potential; E_b is the backward peak potential; j_f is the forward current density; j_b is the backward current density. In the present case, with the voltammogram obtained at a scan rate of 50 mV s^{-1} , these values relative to ethanol oxidation are $E_{\text{onset}} = -847 \text{ mV}$, $E_f = -288 \text{ mV}$, $E_b = -531 \text{ mV}$; $j_f = 6.7 \text{ mA cm}^{-2}$ and $j_b = 1.61 \text{ mA cm}^{-2}$; for multiple-twinned Pd NPs. $E_{\text{onset}} = -847 \text{ mV}$, $E_f = -308 \text{ mV}$, $E_b = -539 \text{ mV}$; $j_f = 1.27 \text{ mA cm}^{-2}$ and $j_b = 0.73 \text{ mA cm}^{-2}$ for single-crystalline Pd NPs. The ratio of j_f to j_b , j_f/j_b , could be used

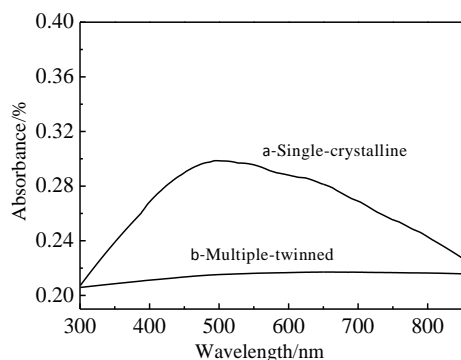


Fig. 5 UV-vis spectra of Pd NPs with single-crystalline structures and multiple-twinned structures

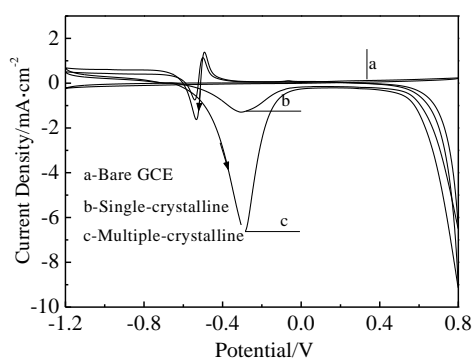


Fig. 6 CVs at bare GCE, the single-crystalline Pd modified GCE, and the multiple-twinned Pd modified GCE

to describe the catalyst tolerance to carbonaceous species accumulation^[20]. Obviously, the ratios of j_f/j_b of multiple-twinned Pd NPs modified electrode (4.16) was higher than of the single-crystalline Pd NPs modified electrode (1.73), revealing the former with better tolerance to carbonaceous species. That is to say, multiple-twinned Pd NPs modified electrode displays a remarkable anti-poisoning property. Furthermore, the current density of the former was 5.27-fold ($6.7/1.27=5.28$) higher than of the latter, revealing better electrocatalytic activity of multiple-twinned Pd NPs as a catalyst. This set of characteristics indicates that the oxidation of ethanol is more favorable with the multiple-twinned Pd NPs. By comparison of micro-morphology between multiple-twinned Pd and single-crystalline Pd, we suspect that high proportion of diffraction planes exposed on the multiple-twinned Pd nano materials is considered the fundamental cause for the increase of the oxidation of ethanol.

3 Conclusions

1) Pd NPs with single-crystalline and multiple-twinned structures have been synthesized selectively by manipulating the reduction rate in a facile visible-light-assisted method.

2) Different Pd nanostructures will provide different performance and useful system for optical or electrochemical applications. The single-crystalline Pd NPs, whose SPR peaks were located at 520 nm and become very broad, exhibit SPR features different from those of multiple-twinned NPs. The multiple-twinned Pd NPs with an average size of 20 nm exhibit a remarkable electrocatalytic activity and anti-poisoning capability for ethanol oxidation and display promise for use in direct ethanol fuel cells.

References

- 1 Nikoshvili L, Shimanskaya E, Bykov A et al. *Catalysis Today* [J], 2015, 241: 179
- 2 Yang Z W, Zhao X, Li T J et al. *Catalysis Communications*[J], 2015, 65: 34
- 3 Wen M, Takakura S, Ku K F et al. *Catalysis Today*[J], 2015, 242: 381
- 4 Wang P, Zhang G, Jiao H et al. *Applied Catalysis A General* [J], 2015, 489: 188
- 5 Peter T, Olivier H, Alain T. *Sensors Actuators*[J], 2001, 74: 168
- 6 Huang R, Wen Y H, Shao G F et al. *RSC Advances*[J], 2014(4): 7528
- 7 Carrera-Cerritos R, Fuentes-Ramírez R, Cuevas-Muñoz F M et al. *Journal of Power Sources*[J], 2014, 269: 370
- 8 Sreedhala S, Sudheeshkumar V, Vinod C P. *Nanoscale*[J], 2014(6): 7496
- 9 Tang Y G, Richard E E, Zou S Z. *Nanoscale*[J], 2014(6): 5630
- 10 Zhang B, Dai W, Ye X C et al. *Angewandte Chemie Interna-*

- tional Edition [J], 2006, 45: 2571
- 11 Navaladian S, Viswanathan B, Viswanath R P. *Nanoscale Research Letters* [J], 2009, 4: 181
- 12 Rojas J V, Castano C H. *Radiation Physics and Chemistry*[J], 2012, 81: 16
- 13 Bera R K, Raj C R. *Journal of Photochemistry and Photobiology A: Chemistry*[J], 2013, 270: 1
- 14 Xiong Y J, McLellan J M, Chen J Y et al. *Journal of the American Chemical Society*[J], 2005, 127: 17 118
- 15 Chen H Y, Gao Y, Zhang H R et al. *Journal of Physical Chemistry B* [J], 2004, 108(32): 12 038
- 16 Zhang S H, Jiang Z Y, Xie Z X et al. *Journal of Physical Chemistry B* [J], 2005, 109: 9416
- 17 Creighton J A, Eadon D G. *Journal of the Chemical Society, Faraday Transactions*[J], 1991, 87: 3881
- 18 Hirsch L R, Stafford R J, Bankson J A et al. *Proceedings of the National Academy of Sciences USA* [J], 2003, 100: 13 549
- 19 Liu J, Ye J, Xu C et al. *Electrochemistry Communications* [J], 2007, 9: 2334
- 20 Zhao G Y, Xu C L, Guo D J et al. *Journal of Power Sources* [J], 2006, 162: 492

单晶和多重孪晶钯纳米粒子的可见光简易合成及其光、电性能

谭德新¹, 王艳丽², 甘颖¹

(1. 安徽理工大学, 安徽 淮南 232001)

(2. 安徽理工大学博士后科研流动站, 安徽 淮南 232001)

摘要: 以氯化钯(PdCl₂)为金属前驱体, 利用简易可见光辅助法制备具有单晶和多重孪晶结构的钯纳米颗粒。借助高分辨透射电镜(HRTEM), 可见分光光度计以及循环伏安法研究了钯纳米粒子纳米结构和电化学性质。结果表明, 不同纳米结构的形成取决于还原速率的控制。与多重孪晶结构的钯纳米颗粒不同, 单晶钯纳米粒子在可见光区域表现了表面等离子共振吸收峰。通过比较单晶和多重孪晶钯纳米粒子氧化过程的电化学参数, 表明多重孪晶钯纳米粒子对乙醇有较好的电催化活性和抗中毒能力。

关键词: 纳米粒子; 光学性质; 电化学性质; 节能灯

作者简介: 谭德新, 男, 1977年生, 博士, 副教授, 安徽理工大学化学工程学院, 安徽 淮南 232001, 电话: 0554-6668485, E-mail: tdxin@163.com